

# Encounter Rates in Zooplankton

L. Dzierzbicka-Głowacka

Institute of Oceanology, Polish Academy of Sciences, Powstańców Warszawy 55, PL-81-712 Sopot, Poland

Received: June 8, 2005

Accepted: November 23, 2005

## Abstract

The influence of turbulence (turbulent kinetic energy dissipation) on predator-prey interactions in zooplankton is discussed with respect to the combined effect of the choice of the turbulent length scale, and size and velocity of predator and prey concentration on the encounter rate. The significance of correct scaling to the turbulent encounter velocity is demonstrated, with three different definitions being considered: the average prey separation, the Kolmogorov scale, and the predator's reactive distance. Numerical investigations using these different definitions of scale were carried out to find the convergence conditions and the behaviour of the scale values for 5-10 mm fish larvae which feed off copepod nauplii in the  $10^4$ - $10^5$   $m^{-3}$  concentration range. The choice of the turbulent length scale is not important for small predator body sizes  $<5$  mm and high prey concentrations in the  $10^7$ - $10^8$   $m^{-3}$  range, which are reasonable prey densities for a 1-3 mm copepod (i.e. algae and protozoans). Also in the quasi-laminar regime of water flow ( $l=2\pi\eta$ ) and high prey concentrations, the choice of correct scaling is not important. Predators of any body size will forage in such a regime immovably (swimming velocity  $v \approx 0$ ). However, for large larval lengths  $>10$  mm and prey concentrations  $<10^6$   $m^{-3}$ , the scale can be defined as the average prey separation or as the predator's reactive distance. The effect of turbulence on the encounter rate decreases with the increasing size and velocity of the predator and with prey concentration. A simple one-dimensional prey-predator ecosystem model in the upper mixed layer is presented, which examines the relative importance of turbulence to growth in planktonic consumers. This effect is less for low prey densities  $<10^4$   $m^{-3}$ , when the initial predator biomass and constant growth rate term have a decisive influence. However, the effect of turbulence on the characteristics investigated increases with rising prey density, in which case the controlling factor is encounter rate and in the case of prey concentration, diurnal migration.

**Keywords:** turbulence, encounter rate, growth rate, prey, predator

## Introduction

The influence of small-scale turbulence on predator-prey interactions in plankton has received a great deal of attention in recent years. The intensive, worldwide research efforts of the 1980s and 1990s provided incontrovertible evidence that the growth of predators - from larval fish to herbivorous copepods - is dependent on small-scale turbulent mixing. Much of this research stems from the work of [1], who suggested that small-

scale turbulence increases planktonic predator-prey contact rates because turbulent fluid motion increases the velocity difference between predators and their prey. Whereupon many papers appeared on the positive influences of turbulence on predator-prey encounters and the potential negative influences of turbulence on organism behaviour [2, 3]. In any case, the modeling of encounter rates and predator growth assumed that both zooplankton and phytoplankton distributions were random in space and time [e.g. 4, 5, 6, 7, 8], because small-scale turbulent process were regarded as homogenizing factors. [1] assumed a simple model in which behaviour of both prey

---

\*e-mail: dzierzb@iopan.gda.pl

and predator is defined using linear swimming. Therefore, in some cases the [1] formula can be unrealistic (but not necessarily) because predators' perception fields are spherical [9]. Subsequent modeling exercises have incorporated 'random walk' types of behaviour. These latter attempts [10, 11] were again purely theoretical, not applied to any real predators, and very difficult for the non-mathematician to understand, apply and test. The effect of turbulence on encounter rates for predators and prey with other behavioural patterns (e.g. ambush predators and suspension feeders which generate feeding currents) was examined by [7]. They formulated simple and general models of prey encounter rates, taking into account the behaviours and motility patterns of both prey and predator as well as turbulent fluid motion. Using these models they determined the levels of turbulence (as the dissipation rate) at which ambient fluid motion is important in enhancing prey encounter rates for various types of predators (e.g. ambush and cruise predators, suspension feeders). Generally, turbulence has the largest effect on prey encounters for predators with low motility and long reaction distances. In addition, turbulence is most important for meso-sized (mm to cm) predators but is insignificant for smaller and larger predators. Turbulence is widely recognized as enhancing contact rates between planktonic predators and their prey [12]. Their conceptual approach is somewhat similar to that of [7]. [12] evaluated the effect of intermittent turbulence and the potential effects of zooplankton behavioural responses to small-scale phytoplankton patchiness on predator-prey encounter rates. Their results indicate that the effects of turbulence on encounter rates is about 35% less important when intermittently fluctuating turbulent dissipation rates are considered instead of a mean dissipation value.

On the basis of a series of models, [5] examined the relative importance of small-scale patchiness and turbulence to growth and recruitment in plankton consumers. By considering the predator swimming diffusion in their models, they demonstrated that, at intermediate levels, physical turbulence causes patch dissipation and reduced growth, whereas at higher levels it causes growth to be restored to the original, low-turbulence values as a result of increased encounter velocities. Using empirical model simulations, [6] evaluated the contribution of wind- and tide-induced small-scale turbulence on encounter rates between larval fish and copepod nauplii. Prey concentration in relation to larval fish swimming speeds were important parameters in encounter rates. They found that the frequency of contacts between larval fish and their prey could be underestimated by one order of magnitude, if one failed to consider the influence of small-scale turbulence when the prey concentration was less than 35 prey  $l^{-1}$ . Neither [4] nor [6] took into consideration either the vertical profile of the turbulent intensity through and below the pycnocline, or the decrease in tidally generated turbulence away from the bottom. However, the vertical profile of turbulence intensity and its potential effect on encounter rates could be important in understanding the influence of

turbulence on larval fish feeding. [13] examined the relationship between larval cod and haddock feeding success and turbulent dissipation in a stratified water column. Observed feeding ratios for three size classes of larvae were compared with estimated ingestion rates using the [1] predator-prey encounter rate model. Feeding ratios were relatively low in the early morning following darkness, when the wind speed was low, but increased by a factor of 12-13 by noon and evening, when the wind speed doubled. Comparison of depth-specific feeding ratios with estimated ingestion rates, derived from turbulence-affected contact rates, were generally reasonable after allowing for an average gut evacuation time (4h), and in many cases the observed and estimated values had similar profiles. All the models of turbulence encounter rates (including [1] equation) assume that on planktonic encounter scales the turbulence is homogeneous and isotropic. [1] results only pertain to encounter rates, not capture rates; hence one can only derive estimates for ingestion rates.

In short, we can no longer investigate the environmental conditions governing the behaviour of plankton without taking into account the fact that their life processes are affected to a considerable extent by the turbulent mixing that homogenizes the uniform fine structure layers.

In this paper I address two main aspects of this continuing debate. Firstly I present a detailed analysis of the combined effect of the choice of the turbulent length scale, predator size and velocity, and prey concentration with respect to turbulence on the prey-predator encounter rate and, therefore, the predator growth rate. It is important to investigate and identify the critical factors in mathematical models of pelagic communities, since zooplankton may play a significant role in marine ecosystems as a top-down regulator. Secondly, I present a simple one-dimensional prey-predator ecosystem model, which shows that turbulence either enhances or reduces predator growth rates depending on its strength. This mathematical model has been used to make a numerical investigation of vertical distributions of predator biomass and prey concentration in the upper homogeneous layer of the sea. The encounter rate is explained in section 2, the prey-predator model is described in section 3, whereas the data from the simulations are presented in section 4, before they are finally discussed in section 5.

### Definition of Encounter Rate

In the ocean the encounter rate is governed by two kinds of processes - behavioural,  $E_B$ , and hydrodynamic processes resulting from water movements. The first condition emerges from the ability to perform autonomous movements (swimming). The second one can be divided into the processes of floating and turbulent mixing, affecting not only aggregation processes but also the speed of the predator's movement with respect to its prey. If we denote this influence by  $E_T$ , we can write:  $E = E_B + E_T$  [7, 12]. The behavioural encounter rate,  $E_B$ , is usually taken

to be that proposed by [14], under the assumption that the speed of the predator,  $v$ , exceeds that of the prey,  $u$ :

$$E_B = \pi Z_p d^2 \left( \frac{u^2 + 3v^2}{3v} \right) \quad \text{for } v > u \quad (1)$$

where  $d$  is the predator's contact radius (i.e. the maximum distance at which the predator can perceive prey), and  $Z_p$  is the prey concentration. On the other hand, the encounter rate due to turbulence  $E_T$ , was expressed by [1]:

$$E_T = \pi Z_p d^2 w, \quad (2)$$

where  $w$  is the linear orbital velocity of turbulent eddies (the turbulent velocity).

[1] suggested that small-scale turbulent motions could also increase behavioural predator-prey contact rates. In essence, they proposed that the relative velocity term of the original [14] model be revised to include a contribution to the relative motion of predator and prey made by microscale turbulence. They accomplished this by rewriting  $V = (u^2 + 3v^2)/3v$  as the relative velocity component of a larval fish to its prey:

$$V = \frac{u^2 + 3v^2 + 4w^2}{3(v^2 + w^2)^{0.5}} \quad (3)$$

Hence, the encounter rate, between predator and prey,  $E$ , can be derived from the equation:

$$E = \pi Z_p d^2 \frac{u^2 + 3v^2 + 4w^2}{3(v^2 + w^2)^{0.5}} \quad (4)$$

[10] suggested a revision of the [1] formulation in order to prevent a breach of [14] original assumption of a uniform predator speed distribution. Evans's formulation is:  $V = (u^2 + v^2 + 2w^2)^{0.5}$ . Evans reported that the two formulations differ by only 6% when  $u = v$ .

Eq. (1) assumes that the predator is swimming and searching for food continuously. However, fish larvae, and most other cruise predators, allocate their time during the day to searching and non-searching activities (Table 1 in paper [15]). As a consequence, if Eq. (1) is used to calculate daily encounter rates, it will give biased results, unless the fraction of time spent searching is included in the calculation. [15] obtained the encounter rate for a pause-travel predator as:

$$E = \pi Z_p d^2 f(2/3R + 1.4\tau w) \quad (5)$$

where  $f$  and  $\tau$  are the pause frequency and pause duration, respectively. Note that in a pause-travel predator, the encounter rate is independent of the swimming velocity. According to [7], the relevant velocity is that immediately before contact; i.e.  $d = r_1 + r_2$  [10]. Inserting the expres-

sions for turbulent velocity and setting  $v = 10^{-6} \text{ m}^2\text{s}^{-1}$  yields [7]:

$$\begin{aligned} \text{for } d < \eta & \quad E_T = 4.2 \pi Z_p \varepsilon^{0.5} (r_1 + r_2)^3 \\ \text{for } d > \eta & \quad E_T = 1.37 \pi Z_p \varepsilon^{1/3} (r_1 + r_2)^{7/3} \end{aligned}$$

where  $r_1$  is the radius of the capture volume (i.e. the volume swept by the copepod's food collecting appendages),  $r_2$  is the prey radius.

[16] determined the perception distance,  $d$ , for larval haddock as a function of body length,  $d_o$ , to be  $2/3\pi(0.75d_o)^2$ . However, [17] determined values of  $d$  equal to  $1.1d_o$ , and the high estimate of swimming speed as:  $\log v \text{ (cm s}^{-1}\text{)} = 1.07 \log d_o \text{ (mm)} - 1.11$ . A predator's reactive distance depends on its prey perception capabilities; be it strength of its eyesight for larval fish, or the sensitivity of its sensory satae to hydromechanical signals for copepods after [18]. Components of foraging behaviour for different species of larval fishes employing either pause-travel (PT) or cruise (C) search behaviour (i.e. reactive distance,  $d$ , swimming activity: percentage of total observation time spent swimming; swimming velocity: swimming speed during individual swimming events,  $v$ ) are given in Table 1 in [15] paper. [15] obtained the reactive distance  $d$  (cm) and swimming velocity  $v$  (cm s<sup>-1</sup>) for cruise and pause-travel fish larval predators as functions of larval lengths  $d_o$  (cm).

The regressions are:

pause-travel predators

$$\log d = -0.163 + 0.717 \log d_o, \quad \log v = -0.050 + 0.26 \log d_o$$

cruise predator

$$\log d = -0.73 + 0.931 \log d_o, \quad \log v = 0.054 + 1.461 \log d_o$$

The turbulent velocity,  $w$ , also called turbulent encounter velocity and encounter velocity below, was parameterized by [1] as:

$$w = 1.9(\varepsilon l)^{1/3} \quad (6)$$

where  $\varepsilon$  is the dissipation rate of turbulent kinetic energy and  $l$  is the characteristic length scale of turbulent eddies. Because the water motion differs below and above the Kolmogorov length scale we should consider  $\eta$  ( $\eta = (v^3/\varepsilon)^{0.25}$ , where  $v$  is the kinematic viscosity, c.  $10^{-6} \text{ m}^2\text{s}^{-1}$ ) describing viscous effects smoothing out turbulent fluctuations. The equations relating turbulent velocity  $w$  and  $\varepsilon$  are also different. Thus the encounter rates due to turbulence should be different. The velocity differences due to fluid motion between two points separated by distance  $l$  is:

$$\text{for } l < \eta \quad (19) \quad w = 0.42 l(\varepsilon/v)^{0.5}$$

$$\text{for } l > \eta \quad (20) \quad w = 1.37(\varepsilon l)^{1/3}$$

where  $(\varepsilon/v)^{0.5}$  is the sub-Kolmogorov scale fluid shear rate. [21] have shown that Eq. (6) is valid considerably below  $\eta$  ( $l \ll \eta$ ).

However, there has been much debate in the literature regarding the correct definition of  $l$ .

Most often,  $l$  has been defined as average prey separation [2, 4, 6, 22, 23, 24]. This distance can be estimated as  $0.55 Z_p^{-1/3}$ , if one assumes that the prey is randomly distributed [25] and as  $Z_p^{1/3}$  [13]. From this evaluation the maximum separation distance between predator and prey is equal to  $\sqrt{3}/2 Z_p^{-1/3}$ . [26] suggested that  $l$  may be defined as the Kolmogorov scale ( $l = 2\pi\eta$ ), whereas [5] assumed it to be equal to the eddy separation distance ( $l = 0.1$  m). Most recently, several authors have suggested that  $l$  should be defined as the predator's reactive distance ( $l = d$ ) [2, 7, 10, 12, 15, 27]. Encounters occur between predators and prey, so the distance must be concerned with the separation between these two distinct micro-organisms, whereas average prey separation does not depend on the predator after [28]. [29] experimentally shows that predator-prey encounters scale as  $d^{7/3}$ , which can only come about if  $l=d$  in Eq. (6). It is interesting to consider the consequences of using the different values of  $l$  in this paper. An example may illustrate the significance of the choice of the length scale (see section 4).

In this paper, the turbulent encounter velocity is given by the expression Eq. (6) of [1], where the relation of the mean rate of energy dissipation,  $\varepsilon$ , at depth  $z$  to wind speed,  $U_{10}$ , in the upper homogeneous layer of the sea is taken from [3]:

$$\varepsilon = 5.82 \times 10^{-9} \frac{U_{10}^3}{z} \quad (7)$$

Here, the energy dissipation given by Eq. (7) is used for  $z > 1/3 H_s$ , where  $H_s$  is the significant wave height. However, for  $z < 1/3 H_s$ ,  $\varepsilon$  is constant according to [30]. The significant wave height is a function of wind speed [31]:

$$H_s = 1.6 \times 10^{-3} \frac{U_{10}^2}{g} \left( \frac{gX}{U_{10}^2} \right)^{0.5} \quad (8)$$

Where  $g=9.81 \text{ ms}^{-2}$  and  $X$  is the wind fetch. Assuming  $X = 100 \text{ km}$  we obtain  $H_s = 0.8 \text{ m}$  for  $U_{10} = 5 \text{ ms}^{-1}$ ,  $H_s = 1.62 \text{ m}$  for  $U_{10} = 10 \text{ ms}^{-1}$ ,  $H_s = 2.42 \text{ m}$  for  $U_{10} = 15 \text{ ms}^{-1}$  and  $H_s = 3.23 \text{ m}$  for  $U_{10} = 20 \text{ ms}^{-1}$ .

Dissipation increases as a cubic function of wind speed and decreases with increasing depth, while the turbulent velocity increases only as the cube root of  $\varepsilon$ . In the upper part of the surface mixed layer,  $\varepsilon$  reaches large values ( $\varepsilon = 17.46 \times 10^{-9} U_{10}^3 / H_s$ , for  $z < 1/3 H_s$ ), which falls substantially with depth according to Eq. (7) for  $z > 1/3 H_s$ ; however, in the lower layer, this decrease gradually declines (Fig. 1).

### Changes in the Zooplankton Concentration Field

The application of turbulent diffusion equations to the modeling of concentrations of herbivorous zooplankton, which in turn are fed upon by larval fish and

carnivorous Copepoda, is a task more complex than the modeling of the hydrodynamically passive phytoplankton. Considering the minute sizes of this zooplankton, we can assume, without committing too serious an error, that turbulent mixing affects ambush-type microzooplankton in the same way as phytoplankton. However, when modeling zooplankton with a cruise-type behaviour, this assumption has to be rejected, because this zooplankton is capable of active movement. Relations between predator and prey are more complex and the foraging process as a component of the source function cannot be defined in the same way as that of phytoplankton, because the principal factor governing it is the encounter rate.

A simple 1D prey-predator model which examines the relative importance of turbulence to growth in planktonic consumers is presented here. Horizontal homogeneity is assumed with the consequence that all horizontal gradients (advective terms) vanish. Fundamental to the present modeling study is the assumption of an absolutely stable vertical distribution of the average sea water density. This means that the mean density and salinity of the water increases and the mean temperature falls with depth. Therefore, the hydrodynamic state of mass transfer and exchange in the various intervals of a stably stratified density distribution can be defined by the vertical distribution of the square of the Väisälä-Brunt frequency.

This mathematical model on which the numerical simulations in the upper homogeneous layer are based, consists of equations for mass (here mass=weight in  $\mu\text{gC}$ ),  $W_p$ , numbers,  $Z_p$ , of a herbivorous copepods at one specific development stage (nauplii); where prey biomass  $Z = \sum W_p Z_p$  [32, 33] and predator biomass,  $B$ :

$$\frac{\partial W_p}{\partial t} = \text{ING} - \text{FEC} - \text{MET} \quad (9)$$

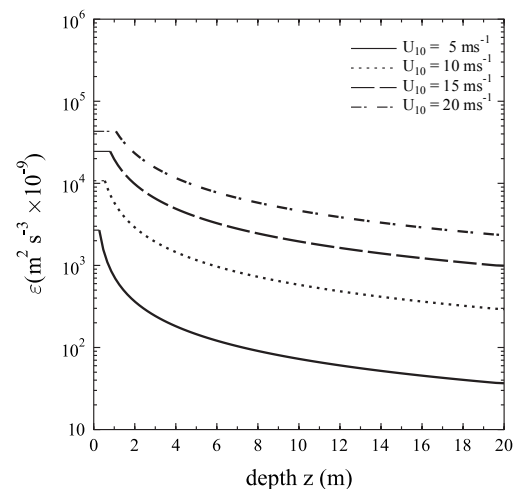


Fig. 1. Turbulent kinetic energy dissipation rate,  $\varepsilon$ , as a function of depth,  $z$ , at four values of wind velocity:  $U_{10} = 5, 10, 15$  and  $20 \text{ m s}^{-1}$ .

$$\frac{\partial Z_p}{\partial t} = \frac{\partial}{\partial z} \left( K_z \frac{\partial Z_p}{\partial z} \right) + \text{MIG} - \text{PRED}_Z \quad (10)$$

$$\frac{\partial B}{\partial t} = \frac{\partial}{\partial z} \left( K_z \frac{\partial B}{\partial z} \right) + gB - \text{PRED}_B \quad (11)$$

If  $W_o$  is the mass of the naupliar stage at which feeding starts and  $W_n$  is the mass of the adult, then for each cohort relations of the form  $\text{EGG} = f(\text{Phyt}, Z_n, W_n/W_o)$  indicate the requirements for some function defining recruitment EGG in terms of food available *Phyt*, adult numbers  $Z_n$  and the ratio of adult to naupliar mass (see Appendix 1). Eq. (9) determines the change in mass as the sum of gains (ingestion, ING) and losses (zooplankton fecal pellets, FEC and metabolism, MET) of energy. Eq. (10) represents the effects of turbulent diffusion,  $K_z$ , diurnal migration, MIG, and predation,  $\text{PRED}_Z$ , on prey concentration, assuming that all death is due to predation. The processes influencing the source/sink terms (i.e. ING, FEC, and MET) are given in Appendix 1 and a detailed description is presented in [32, 33]. The migration process is described in a day-night cycle as  $\text{MIG} = f(t, z) \partial Z_p / \partial z$ , and  $f(t, z) = 1 + a_w \cos(\omega(t - t_o))h(z)$  is a time and space varying vertical migration velocity, where  $a_w$  is the relative amplitude of zooplankton concentration changes,  $t_o$  is the time in which the maximum zooplankton concentration occurs (see Table 1) and  $\omega = 2\pi / T$  ( $T=24$  h) and  $h(z)$  is the vertical distribution of zooplankton.  $\text{PRED}_Z$  represents the losses incurred by  $Z_p$  as a result of predation. Its magnitude can be determined from the biomass of predator  $B$  on the assumption that the loss incurred by prey concentration  $Z_p$  is proportional to the increase in the predator biomass (here  $\text{PRED}_Z = \alpha g B / W_p$ ; where  $g$  is the predator growth rate and assumed  $\alpha=5/4$ ; this means that 80% of ingested food is contributed to predator growth and 20% is voided as fecal pellets and excreted material which is assumed to be lost immediately). The predation term in Eq. (10) depends inversely on  $W_p$ ; it is harder for the predators to capture the larger forms of nauplii. Such defined  $\text{PRED}_Z$  includes food (prey) selection.  $\text{PRED}_B$  is predation by higher-order species. The predator growth rate,  $g$ , when predator is food limited, is linearly related to the encounter rate,  $E$ , by [5]:

$$\begin{aligned} g &= g_1 E + g_2 & \text{for } Z < Z_{\max} \\ g &= g_{\max} & \text{for } Z \geq Z_{\max} \end{aligned} \quad (12)$$

where  $g_1$  is the proportionality parameter between growth rate and encounter rate and  $g_2$  is the constant growth rate term. Increased encounter rate only leads to increased growth when the predator is food limited and then the first term of Eq. (12),  $g_1$ , has decisive influence on growth rate; if the mean time between prey encounter becomes small, the predator growth rate becomes limited not by prey availability ( $E$  is greater than  $1 \text{ s}^{-1}$  and is un-

likely to lead to an increased ingestion rate and then  $g_1$  is constant), but by parameter  $g_2$  and then the predominant influence has  $g_2$  and  $g \rightarrow g_{\max}$ . In this paper parameters  $g_1$  and  $g_2$  are considered as constants and are chosen such that the growth rate lies in the range  $0 < g < g_{\max}$ . Physical diffusivity,  $K$ , in the ocean pycnocline is related to surface wind speed,  $U_{10}$ , through the turbulent kinetic energy dissipation rate,  $\epsilon$  by [35]:

$$K(z) = \Gamma \epsilon N^{-2}(z) \quad (13)$$

where  $N$  is the Väisälä-Brunt parameter and is computed according to the vertical structure of the water column and  $\Gamma$  is an efficiency coefficient taking various values: according to [36],  $\Gamma \approx 0.2$ , and according to Osborn himself [36]. This estimate may be transformed to the simple relation  $P_b/\epsilon = 0.2$  giving  $e_3 = 5.8$  and is equivalent to  $Ri^{\text{st}} = 0.152$ ; where  $P_b = K(g/\rho_o)\partial\rho/\partial z$  is the buoyancy production,  $Ri^{\text{st}}$  is the steady-state Richardson number and  $e_3$  is an empirical constant for the extended  $k - \epsilon$  model by [37].

### Results of Numerical Investigations

The combined effect of turbulence (the dissipation rate), the choice of the turbulent length scale, and the size and velocity of predator and prey concentrations on the variability of the processes investigated (i.e. the turbulent, predator-prey encounter rate and predator growth), was analyzed in the upper mixed layer (Gdańsk Deep), where 20 m is above pycnocline except summer months [38]. The stability of the water column expressed as buoyancy frequency squared  $N^2$  is in the time ca.  $10^{-3} - 10^{-5} \text{ s}^{-2}$ .

The calculations were carried out for three different  $l$ :  
 case 1:  $l = \sqrt{3} / 2 Z_p^{-1/3}$  for  $Z_p = 10^4, 5 \times 10^4, \text{ and } 10^5 \text{ m}^{-3}$  where  $Z_p$  is the prey concentration, because 5-10 mm fish larvae feed on copepods ( $10-100 \text{ l}^{-1}$ );  
 case 2:  $l = d$  for larval lengths  $d_o = 5.5, 7.5 \text{ and } 9.5 \text{ mm}$ , where  $d$  is the predator's reactive distance, and here,  $d$  is obtained after [16]. These larval lengths are characteristic mainly of the size of saltwater fish (see Table 1 in [15] paper);  
 case 3:  $l = q\eta$  for  $q=1, 3, 6 \text{ and } 9$  where  $\eta$  is the Kolmogorov length scale.

### Encounter Velocity

The influence of the characteristic length scale,  $l$ , on the variability of the encounter velocity,  $w$ , as a function of wind speed,  $U_{10}$ , was studied and for correctness of analysis and clarity of figures, the calculations are presented for two values of the depth: for the top ( $z = 1 \text{ m}$ ) and bottom ( $z = 20 \text{ m}$ ) of the surface mixed layer, knowing that  $w$  falls with depth according to  $\epsilon$ .

The turbulent encounter velocity,  $w$ , decreases as the cube root of depth and increases linearly with wind speed and as the cube root of the length scale  $l$ . In case 1 (Fig. 2A)  $w$ , in the  $0 - 20 \text{ ms}^{-1}$  wind speed range, increases from 0 to c.  $23 \times 10^{-3} \text{ ms}^{-1}$  and to  $18 \times 10^{-3} \text{ ms}^{-1}$  for  $Z_p = 10^4 \text{ m}^{-3}$  and  $10^5 \text{ m}^{-3}$ , respectively, for  $z = 1 \text{ m}$ ; however, for  $z = 20 \text{ m}$ , the value of  $w$  decreases about three times. In cases 2 and 3 the scale  $l$  is independent of prey density,  $w$  assumes values lower than in case 1.

And so, in case 2 (Fig. 2B),  $w$  is reduced by about 30% with respect to case 1. However, in case 3 (Fig. 2C), when  $l$  is defined as the Kolmogorov scale,  $w$  takes the lowest values and is reduced by about 50%. Comparing the turbulent velocity for different choices of the scale  $l$ , the results show that for  $q = 6$  when  $l = f(\eta)$  (case 3) and for  $d_o = 5.5 \text{ mm}$  when  $l = f(d_o)$  (case 2),  $w$  assumes values of around  $11 \times 10^{-3} \text{ ms}^{-1}$ . The calculations also suggest that for small larval lengths  $d_o < 5 \text{ mm}$  and high prey concentrations  $Z_p > 10^7 \text{ m}^{-3}$  the encounter velocity will assume low values in all cases, as in case 3 for  $q < 9$ . Prey concentrations in the  $10^4 - 10^5 \text{ l}^{-1}$  are reasonable densities for prey of a 1-3 mm copepod (i.e. algae and protozoans). However, for large larval  $d_o > 10 \text{ mm}$  and for low prey concentrations,  $Z_p < 10^4 \text{ m}^{-3}$ ,  $w$  will assume high values in the same range in cases 1 and 2. These larval lengths ( $d_o > 10 \text{ mm}$ ) are characteristic mainly of the small sizes of freshwater species (see Table 1 in [15] paper). The results of the calculations suggest that for high  $Z_p$  the water flow becomes quasi-laminar and predator foraging occurs in the stationary regime with a swimming velocity equal to zero, while for low  $Z_p$ , predator foraging depends significantly on the swimming velocity and encounter rate.

### Encounter Rate

Let us now examine the combined effects of prey concentration, turbulent velocity, and larval length and velocity on the encounter rate,  $E$ . The following assumptions were made in the calculations:

1. A high and low estimate of swimming speed was used for the three size classes of larval fish (predator), i.e. 5-6 mm, 7-8 and 9-10 mm;
2. The low estimate,  $v_{min}$ , was based on a laboratory study of cod larvae by (39), where larvae increased their speed from  $0.10 \text{ cms}^{-1}$  for the 5-6 mm size class, to  $0.16 \text{ cms}^{-1}$  for the 7-8 mm and  $0.24 \text{ cms}^{-1}$  for 9-10 mm fish;
3. The high estimate of swimming speed,  $v_{max}$ , was derived by (17);
4. The swimming speed of prey was based on the estimate of (4), who used an average speed of 0.5 body length for *Calanus finmarchicus* nauplii. The mean length of prey estimated from gut contents in this study increased from about 0.2 mm for the 5-6 mm size class, to 0.3 mm for the 7-8 mm, and 0.4 mm for the 9-10 mm fish, corresponding to a prey swimming speed,  $u$ , of 0.010, 0.014 and  $0.020 \text{ cms}^{-1}$ ;
5. The perception distance for larval fishes was based on the estimate by [16].

The encounter rate,  $E$ , as a function of wind speed in the range  $0 - 20 \text{ ms}^{-1}$  was obtained for the given three larval lengths. The calculations are presented for the upper part of the surface mixed layer ( $z = 1 \text{ m}$ ) when  $E$  attains the highest values, which fall with depth according to dissipation by

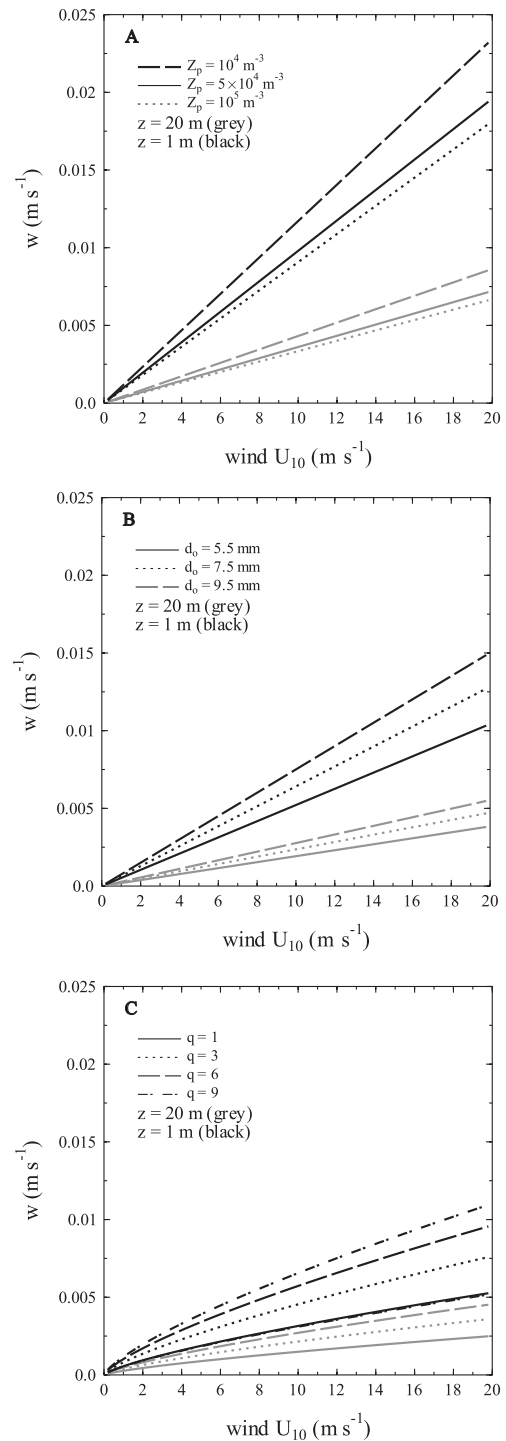


Fig. 2. Turbulent encounter velocity,  $w$ , as a function of wind velocity,  $U_{10}$ , for different spatial scales:  $l = \sqrt{3}/2Z_p^{-1/3}$  (A),  $l = d$  (B) and  $l = q\eta$  (C). The calculations are presented at the upper ( $z = 1 \text{ m}$  - black line) and lower ( $z = 20 \text{ m}$  - grey line) of the surface layer of sea.

turbulent velocity. In all cases, in the lower layer ( $z = 20$  m),  $E$  is reduced by about 75%. The results of numerical investigations demonstrate the predominant influence of the choice of the turbulent length scale on the encounter rate. Hence, an increase in larval size and prey concentration causes an

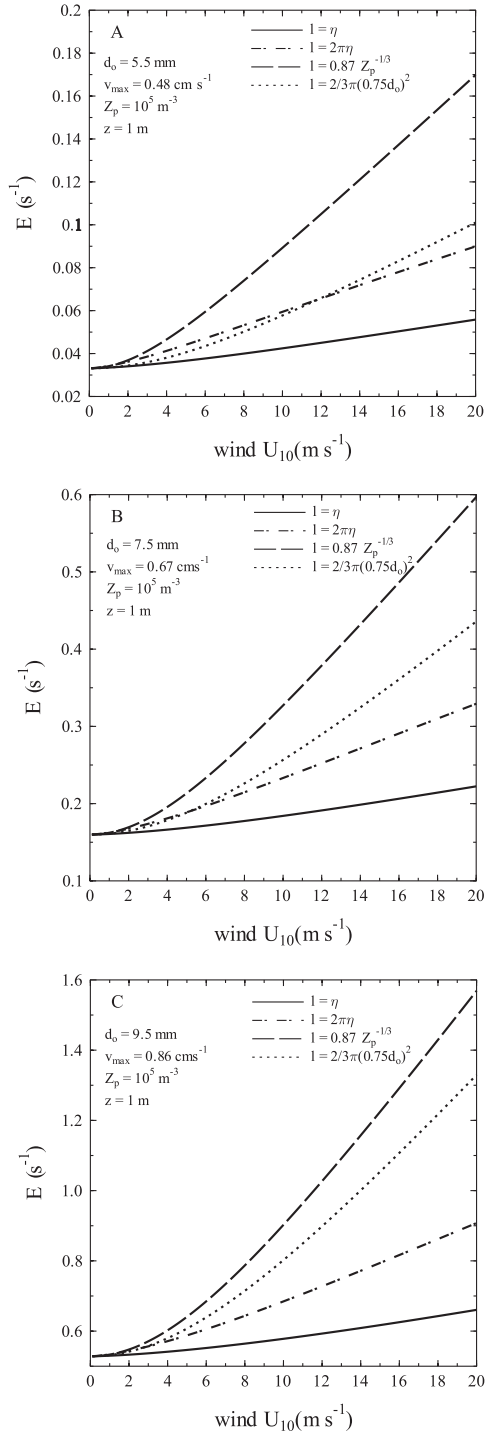


Fig. 3. Encounter rate,  $E$ , as a function of wind velocity,  $U_{10}$ , for different spatial scales,  $l$ , and for different larval lengths  $d_o = 5.5$  mm (A),  $7.5$  mm (B) and  $9.5$  mm (C). The calculations are presented for prey concentration  $Z_p = 10^5 \text{ m}^{-3}$  at the surface ( $z = 1$  m).

increase in the encounter rate. Fig. 3 shows, for a given prey density ( $Z_p = 10^5 \text{ m}^{-3}$ ), the encounter rate,  $E_{d_o}$  when  $l = d_o$ , for the three sizes of larval fish lies in the range  $E_\eta < E_{d_o} < E_{Z_p}$  i.e. between  $E_\eta$  when  $l = f(\eta)$  and  $E_{Z_p}$  when  $l = f(Z_p)$ . For small larval sizes  $E_d \approx E_\eta$ ; however, for large ones  $E_{d_o} \approx E_{Z_p}$ .

Fig. 4A shows, the influence of the predator velocity,  $v$ , on the encounter rate,  $E$ , as a function of the turbulent velocity,  $w$ , in the  $0-0.016 \text{ ms}^{-1}$  range, under the assumption that optimal predator velocities are equivalent to the given three larval lengths. This influence increases with decreasing turbulent velocity.

The range of variability of  $E$  is considerably higher for  $v_{\min}$  than for  $v_{\max}$ . For a high turbulent velocity,  $E$  independent of predator velocity, i.e.  $E$  assumes values similar for an optimal  $v$ . However, for a low one,  $E$  is much less for  $v_{\min}$  than for  $v_{\max}$  and the difference between  $E_{v_{\min}}$  and  $E_{v_{\max}}$  increases with decreasing larval size.

In this paper, a normalized encounter rate,  $E/E_{U_{10}=0}$  (i.e. encounter rate,  $E$ , to behavioural encounter rate,  $E_B = E$  for  $U_{10}=0$ , ratio) in the  $0 - 20 \text{ ms}^{-1}$  wind speed range also was obtained for the analysis of the effect of turbulence on  $E$ . The  $E/E_{U_{10}=0}$  ratio describes how many times  $E = E_B + E_T$  increases in relation to  $E_B$  with wind speed. The calculations demonstrate (see Fig. 5) that a decline in  $d_o$  causes an increase in the effect of turbulence on the encounter rate. When  $l$  is defined as the predator's reactive distance  $l = d = f(d_o)$ , the decrease in  $E/E_{U_{10}=0}$  with increasing  $d_o$  is linear (i.e. for  $U_{10} = 20 \text{ ms}^{-1}$ ,  $E/E_{U_{10}=0} = 3, 2.75$  and  $2.5$  for  $d_o = 5.5, 7.5$  and  $9.5$  m, respectively). However, in other cases, this decrease is logarithmic, i.e. for larger and larger larval sizes it grows less. The normalized encounter rate assumes comparable values when  $l = d$  and  $l = 2\pi\eta$  for  $d_o = 5.5$  mm and when  $l = d$  for  $d_o \approx 10$  mm and  $l = f(Z_p)$  for  $Z_p = 10^5 \text{ m}^{-3}$ . Fig. 5B shows, for a defined larval size,  $E/E_{U_{10}=0}$  is constant when  $l = f(\eta)$  and  $l = f(d_o)$ , but when  $l = f(Z_p)$ , this ratio decreases with increasing  $Z_p$ . In this situation, the intensity of the effect of turbulence on the encounter rate does not change when  $l = f(\eta)$  and  $l = f(d_o)$ ; however, when  $l = f(Z_p)$ , any increase in the prey density,  $Z_p$ , causes this influence to decline.

Analysis of this process shows that the intensity of the effect of turbulence through the turbulent velocity on the encounter rate depends to a high degree on predator velocity. Fig. 4B shows that this intensity considerably increases with decreasing predator velocity and larval size; for  $w = 0.016 \text{ ms}^{-1}$ , and  $d_o = 5.5$  mm for  $v_{\min}$ , the normalized encounter rate is equal to ca. 20, i.e. the encounter rate is ca. 20 times higher than the behavioural encounter rate.

### Predator Growth Rate

Given the relationships in sections 1 and 2 for physically dependent growth and diffusion, we can explore the effects of wind mixing and prey concentrations on the predator growth rate. At first we consider the case of a steady wind at various velocities and examine predator

growth with different initial prey concentrations and for optimal predator velocities. Then we shall examine the case of variable winds, i.e. time-dependent distributions.

The following assumptions were made in the calculation:

1. *Mysis mixta* for earlier stages was used as predator;
2. Maximum growth rate of 0.5-1.5 mg<sub>w.w.</sub> size class of *Mysis mixta* was given by [40] as 0.071 d<sup>-1</sup>; here assumed that mean mass of predator is equal to c. 160 μgC and mean length is equal to  $d_o \approx 7.5$  mm;
3. Growth parameters  $g_1$  and  $g_2$  were chosen such that the growth rate ranges from 0.0 - 0.071 d<sup>-1</sup> (see Table 1);
4. The youngest stages - nauplii of four genera *Pseudocalanus*, *Acartia*, *Centropages* and *Temora*, were used as prey and its mean mass is ca. 0.9 μgC;
5. Growth rates were given by [41] and [42, 43]; here assumed that mean maximum growth rate of prey is ca. 0.08 μgC d<sup>-1</sup>;
6. Here considered the high level of phytoplankton biomass in the spring bloom time, which does not influence the growth rate of copepods, i.e the function  $fil(\{Phyt\}) \rightarrow f_{max}$  in Eq. (15) because the expression  $(\{Phyt\} - \{Phyt_o\}) / (\{Phyt\} - \{Phyt_o\} + k_{phyt}) \rightarrow 1$  (see [33]);

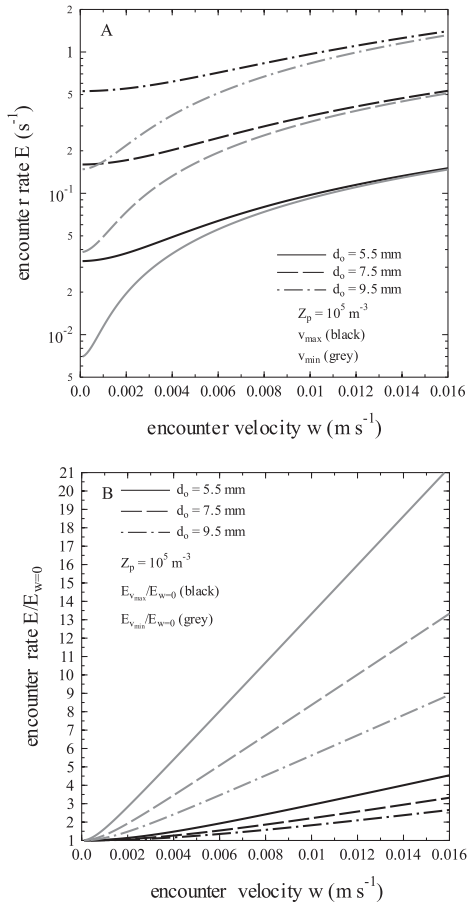


Fig. 4. Encounter rate,  $E$ , (A) and normalized encounter rate,  $E/E_{w=0}$  as a function of turbulent encounter velocity,  $w$ , for two values of predator velocity,  $v_{min}$  (grey line) and  $v_{max}$  (black line). The calculations are presented for the three size classes of larval fishes  $d_o = 5.5, 7.5$  and  $9.5$  mm and for prey concentration  $Z_p = 10^5$  m<sup>-3</sup>.

7. During the numerical experiment (two days in the spring bloom time), growth rate of prey as a function of time and depth is constant and in this situation, the time-vertical changes in prey biomass are caused by prey density; therefore in this case prey concentration

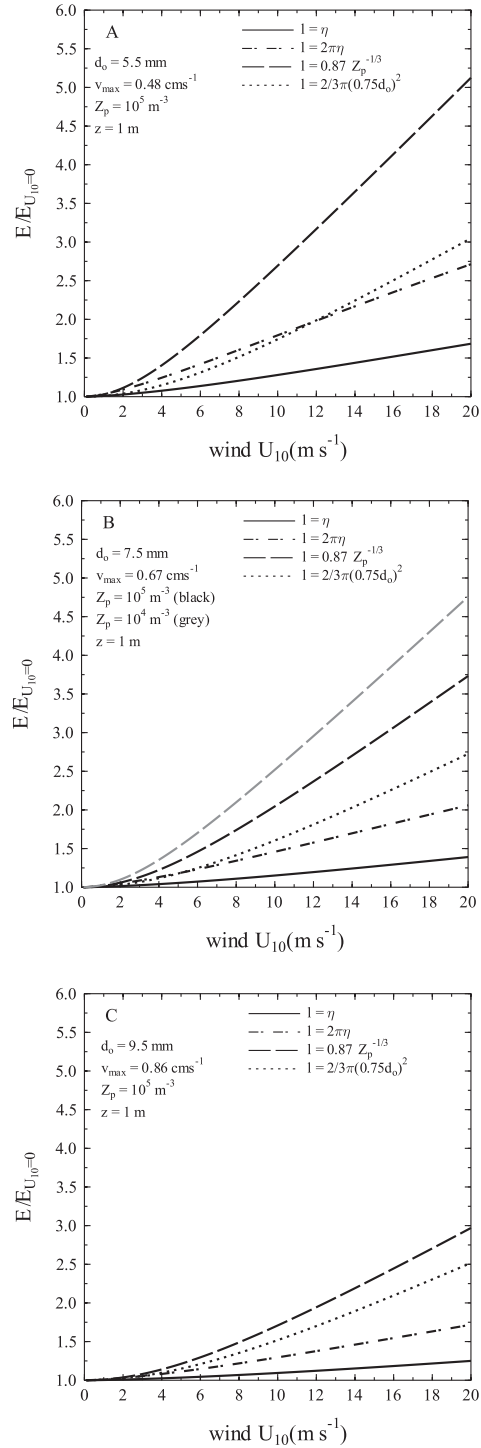


Fig. 5. Normalized encounter rate,  $E/E_{U10=0}$  as a function of wind velocity,  $U_{10}$  for different spatial scales,  $l$ , and for different larval lengths  $d_o = 5.5$  mm (A),  $7.5$  mm (B) and  $9.5$  mm (C). The calculations are presented for prey concentration  $Z_p = 10^5$  m<sup>-3</sup> and in case 2 also for  $Z_p = 10^4$  m<sup>-3</sup> at the surface ( $z = 1$  m).

is presented in Figs 8, 10 and 11;

8. The function describing a vertical distribution of zooplankton was assumed as  $h(z) = -0.003z + 0.03$ , where  $h(z)$  shows slight vertical changes because phytoplankton biomass is high in the spring bloom time insignificantly differs in the 20 m water column;
9. During this numerical experiment (two days), egg production and predation by higher-order species were not considered.

The model was dimensionalized for an optimal predator velocity, three different prey concentrations  $Z_p = 10^4$ ,  $5 \times 10^4$  and  $10^5 \text{ m}^{-3}$  and initial value of predator biomass  $B = 800 \mu\text{gCm}^{-3}$ .

In this paper the characteristic length scale  $l$  in the turbulent velocity (Eq. 5) is defined as the predator's relative distance; i.e.  $l=d$  in the equation for the encounter rate.  $d$  is here obtained after [16] and is equal to about 0.66 cm.

With these parameter values, for three prey concentrations and increasing turbulence (with wind speed up  $18 \text{ ms}^{-1}$ ), Fig. 6. shows the growth rate increases for  $v_{\max}$  from 0.023 to 0.025, from 0.029 to 0.041, and from 0.037 to 0.061  $\text{d}^{-1}$  and for  $v_{\min}$  from 0.022 to 0.025, from 0.023

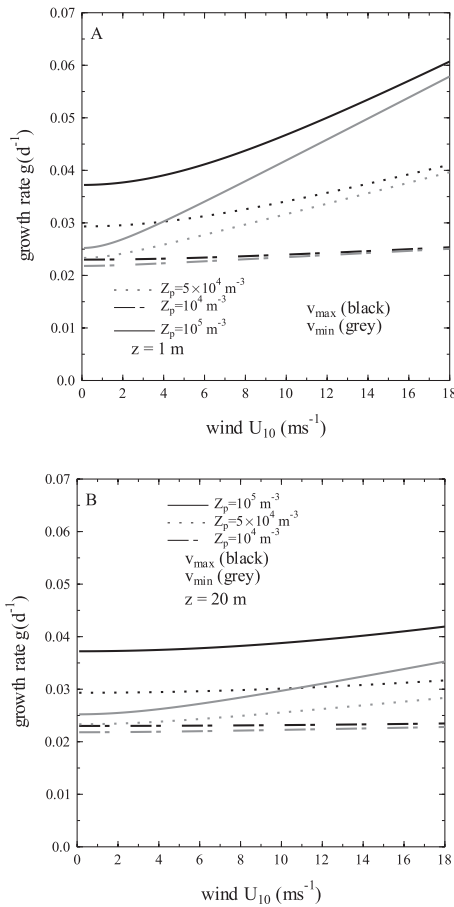


Fig. 6. Predator growth rate,  $g$ , as a function of wind speed,  $U_{10}$ , for three different prey concentrations:  $10^4$ ,  $5 \times 10^4$ , and  $10^5 \text{ m}^{-3}$ , and for optimal predator velocities,  $v_{\max}$  (black line) and  $v_{\min}$  (grey line) at the upper ( $z = 1 \text{ m}$ ) and lower ( $z = 20 \text{ m}$ ) of the surface layer of sea.

Table 1. Dynamic constants in the model.

Symbol	Numerical value	Unit	References
$k_{\text{Phyt}}$	100	$\text{mgC m}^{-3}$	33
$\{Phyt\}_o$	10	$\text{mgC m}^{-3}$	33
$n_e$	0.33		47
$n_f$	0.33		47
$a_w$	0.6		49
$t_o$	3.25 a.m.	h	49
$g_1$	$10^{-6}$		
$g_2$	0.02	$\text{d}^{-1}$	
$\tau$	1		

to 0.039, and from 0.025 to 0.057  $\text{d}^{-1}$  for  $Z_p = 10^4$ ,  $5 \times 10^4$  and  $10^5 \text{ m}^{-3}$ , respectively, in the upper layer ( $z=1\text{m}$ ). However, in the lower layer ( $z=20 \text{ m}$ ), the growth rate increases more slowly with wind speed for  $v_{\max}$  to 0.023, 0.032 and 0.042, for  $v_{\min}$  to 0.022, 0.028 and 0.035  $\text{d}^{-1}$  for  $Z_p = 10^4$ ,  $5 \times 10^4$  and  $10^5 \text{ m}^{-3}$ , respectively.

The calculations made here show significant changes in predator growth in relation to prey concentration. A decrease in food concentration retards the predator growth rate, thus the predator velocity has a greater impact on growth rate as prey concentration increases. Knowing the value of  $g_{p1}$  for  $Z_{p1}$  we can compute  $g_{p2}$  for any value of  $Z_{p2}$  by:  $g_{p2} = (g_{p1} - g_{p2})Z_{p2}/Z_{p1} + g_2$ , and obviously for a given body size  $d_o$ , predator velocity  $v$ , and wind speed  $U_{10}$ , assuming that  $l = d$ .

The time-dependent solution with varying wind (Fig. 7A) reflects the results of the steady wind case. With variable winds from  $0.1\text{--}18 \text{ ms}^{-1}$  assuming an increase and then a decrease in wind speed during 2 days, physical diffusivity is greatest at maximal wind speeds and lowest at minimal wind speeds (Fig. 7B) and in this paper was obtained by Eq. (12) assuming  $N^2 = 0.001 \text{ s}^{-2}$ , it is conformable to the vertical structure of the upper layer in Gdańsk Deep in the spring.  $K$  reaches values about one order of magnitude larger in the upper mixed layer ( $z = 1 \text{ m}$ ) than in the lower one ( $z = 20 \text{ m}$ ). The encounter velocity,  $w$ , (Fig. 7C) ranges from 0 to  $0.012 \text{ ms}^{-1}$  for  $z = 1 \text{ m}$  (black line) and to  $0.004 \text{ ms}^{-1}$  for  $z = 20 \text{ m}$  (grey line), because  $w$  decreases as the cube root of depth while  $K$  decreases linearly. In this case, for  $Z_p = 10^5 \text{ m}^{-3}$  encounter rate lies in the range from  $0.152$  to  $0.44 \text{ s}^{-1}$  for  $z = 1 \text{ m}$  and decreases with depth; however, for  $Z_p = 10^4 \text{ m}^{-3}$ ,  $E$  is order lower.

In the time-dependent case, the predator growth rate,  $g$ , for high wind speeds is high relative to the substantial increase in turbulent encounter velocity (Fig. 8A and B). When the predator is food limited, an increase in predator growth rate is caused mainly by an increase in encounter rate and then, for  $Z_p = 10^5 \text{ m}^{-3}$ ,  $g_1 E > g_2$  and  $g \rightarrow g_{\max}$  for strong winds, but for weak ones  $g_1 E \approx g_2$ ; however, for  $Z_p = 10^4 \text{ m}^{-3}$ ,  $g_1 E \approx g_1 E_B \ll g_2$  and  $g \approx g_2$  (see Fig. 8A and B). The results indicate that any

increase in prey concentration causes the predator growth rate to rise considerably in the upper mixed layer (Fig. 8A), which decreases with depth (Fig. 8B) during high winds. However, when winds are low  $U_{10} < 2 \text{ ms}^{-1}$ , for different values of prey concentrations,  $Z_p$ , and predator velocities,  $v$ , the predator growth rate assumes suitable values according to Eq. (12), which are constant throughout the upper mixed layer because, in this case,  $E = E_B + E_T \approx E_B$ . A decrease in predator velocity causes a decrease in growth rate, which is evidenced by a drop in the encounter rate at low wind speeds. The differences in  $g$  for optimal predator velocities increase with depth for strong winds. Thus, for weak winds they are unaffected by the mixed layer depth (Fig. 8B), because  $E_T \approx 0$  in the whole column water. The distributions shown in Figs (8C and D) demonstrate the changes in predator biomass,  $B$ . In the middle stage of the numerical experiment (between 18 and 36 hours), a substantial growth in predator biomass is observed, mainly for  $Z_p = 10^5 \text{ m}^{-3}$ , which falls slightly in the final stage as result of the decrease in growth rate. This drop is caused by the decline in wind speed. The results indicate that the changes in growth rate with prey concentration and predator velocity exert hardly any influence on predator biomass. They show, moreover, that any increase in the values of  $Z_p$  and  $v$  causes the predator biomass to rise considerably. The differences in predator biomass for optimal predator velocities decrease with declining prey concentration. The numerical investigations suggest that for a low prey density  $Z_o < Z_p \leq 10^4 \text{ m}^{-3}$  (where  $Z_o$  is prey threshold for predator growth), the predator biomass in the upper ( $z = 1$ )

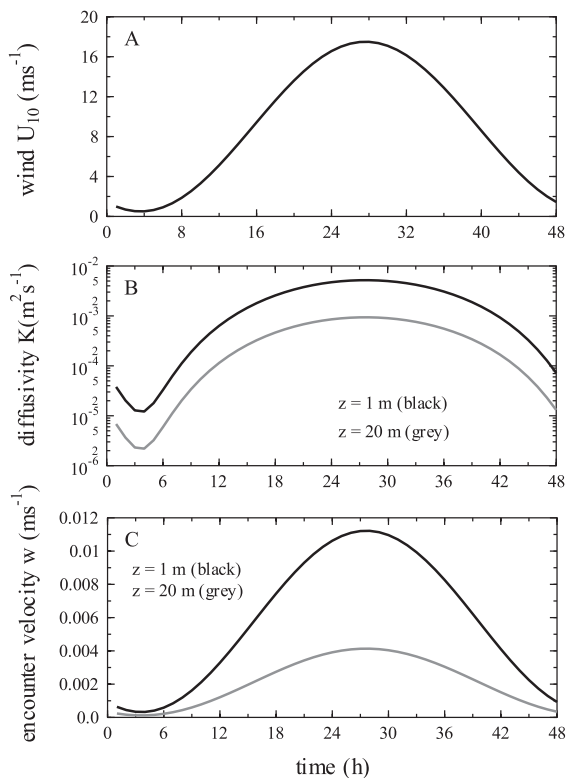


Fig. 7. Effects of temporally varying winds (A) on physical diffusivity (B) and turbulent encounter velocity (C) at the upper (black line) and lower of the surface mixed layer (grey line).

and lower ( $z = 20$ ) layer took similar values throughout the numerical experiment. Hence, the effect of growth rate through prey concentration and predator velocity on predator biomass is very small, because  $E$  is very low and  $g \approx g_2$ . This situation is caused mainly by a fall in prey concentration (Fig. 8F) during this experiment (2 days). In turn, this decrease is created by predation  $\text{PRED}_Z$ . In this case, when the density  $Z_p$  is so low,  $\text{PRED}_Z$  depends mainly on the initial predator biomass and parameter  $g_2$ , which have a decisive influence on the time-vertical distributions of prey concentration (see Fig. 11C). The intensity of this effect on prey concentration declines with increasing  $Z_p$ ; in this case, predator growth rates depend mainly on encounter rate,  $g$ , and diurnal migration,  $\text{MIG}$ , exerting a considerable influence on prey density (Fig. 8E).

The time-dependent vertical distributions of characteristics investigated (predator growth rate, predator biomass and prey concentration) are presented for maximum predator velocity and two prey density  $Z_p = 10^4$  and  $10^5 \text{ m}^{-3}$ . In this model formulation,  $K$  is obtained as above, assuming  $N^2 = 0.001 \text{ s}^{-2}$ , and is shown in Fig. (9) at time  $t = 12, 24, 36$  and  $48 \text{ h}$ . Figs. (10 A) and (11 A) present the changes in the predator growth rate with depth for the same values of time for two prey concentration.  $g$  decreases with depth in the whole water column, but this fall is marked only in the upper mixed layer, mainly at  $t = 24 \text{ h}$  and  $36 \text{ h}$ , when wind speed is very high, in this time,  $g$  lies in the range from  $0.053$  to  $0.061 \text{ d}^{-1}$  ( $g \rightarrow g_{\text{max}}$ ) and  $0.0245$  to  $0.0255 \text{ d}^{-1}$  ( $g \approx g_2$ ) for  $Z_p = 10^5$  and  $10^4 \text{ m}^{-3}$ , respectively. The vertical distributions of predator biomass,  $B$ , reflect the growth rate, showing a decrease with depth and a higher increase with time at high turbulence levels than at low ones (Figs. 10B and 11B). However, the vertical distributions of prey concentration,  $Z_p$ , reflect the diurnal migration  $\text{MIG}$  and predation  $\text{PRED}_Z$  (Figs. 10C and 11C).

The effect of  $\text{PRED}_Z$  on prey concentration is observed mainly for high wind. The increase in predation, resulting from the increased predator biomass as a consequence of the faster growth rate (through encounter rate), causes a fall in the prey concentration. The effect of  $\text{MIG}$  on  $Z_p$  is visible late in the day, when prey translocates to the upper layer; however, in the morning it translocates to the lower layer. Figs 10C and 11C show the combined effect of predation and migration on prey concentration. The predicted effect of  $\text{MIG}$  on  $Z_p$  is much more pronounced when  $Z_p = 10^5$  than when  $Z_p = 10^4 \text{ m}^{-3}$ ; however, the effect of  $\text{PRED}_Z$  on  $Z_p$  is larger for  $Z_p = 10^4$  than for  $Z_p = 10^5 \text{ m}^{-3}$ .

If we assume initial values of  $B = 800 \mu\text{gC m}^{-3}$  and the above principles, an increase in predator biomass is observed from 4% and 11% on the surface of mixed layer to 3% and 7% at depth during the numerical experiment with a drop in prey concentration from about 2% and 6% for  $Z_p = 10^5$  and  $10^4 \text{ m}^{-3}$ , respectively.

## Conclusions

The paper reports numerical results; it gives an analysis of the equation for the encounter rate in zooplankton and the time-dependent vertical distributions of predator growth

rate, predator biomass and prey concentration with variable winds. Using different definitions of scale  $l$ , the numerical investigations were carried out to find the convergence conditions and the behaviour of the scale values. In this paper the significance of the choice of the length scale in

turbulent encounter velocity was demonstrated: three different definitions of  $l$  were taken into consideration - the average prey separation,  $l = f(Z_p)$ , the Kolmogorov scale,  $l = f(\eta)$ , and the predator's reaction distance,  $l = f(d_o)$ . Analysis of these numerical studies indicates that, for a predator

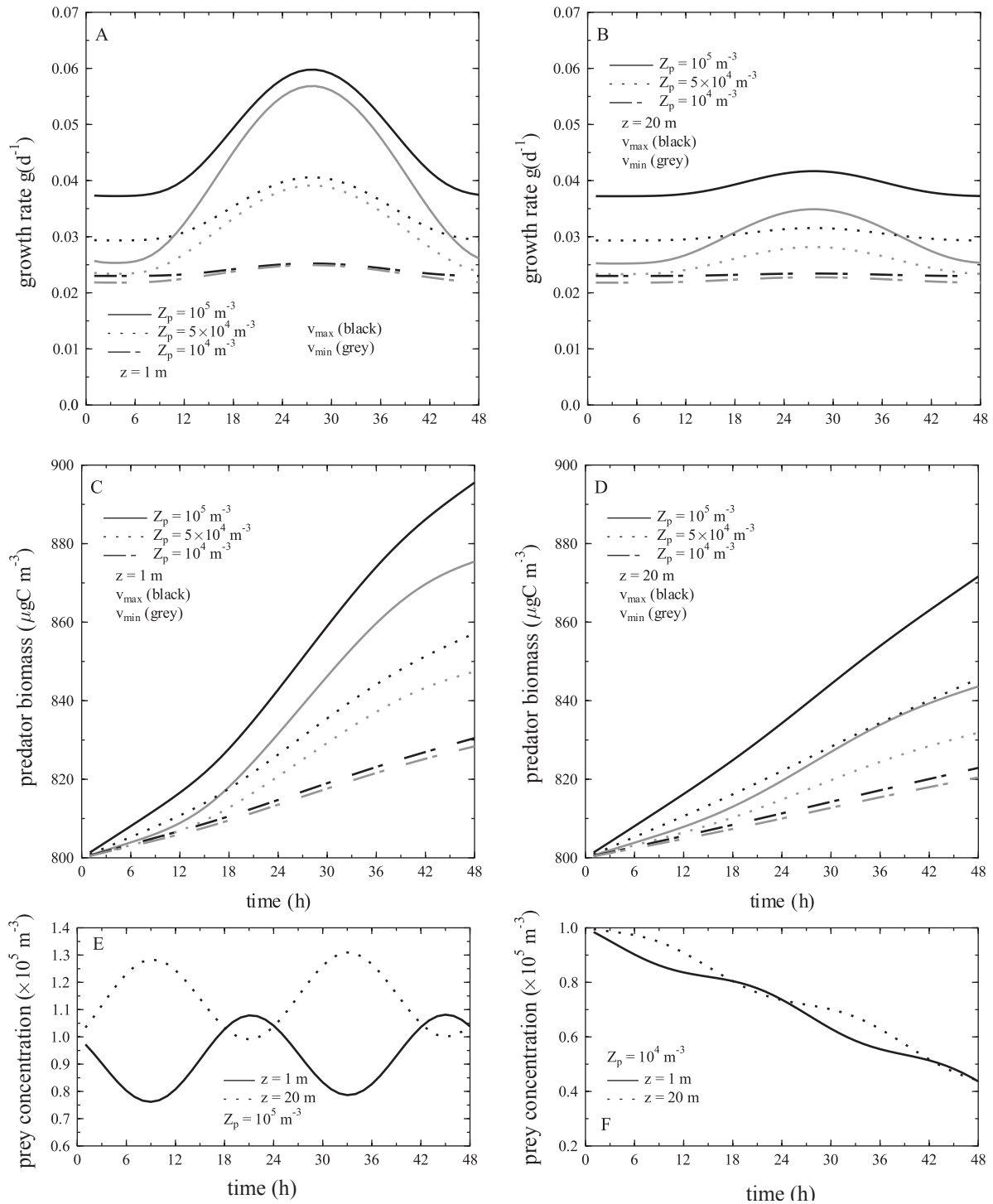


Fig. 8. Temporal changes in predator growth  $g$  rate, (A) and (B) and predator biomass  $B$ , (C) and (D) with varying wind for three different initial prey concentrations:  $10^4$ ,  $5 \times 10^4$ , and  $10^5$  m<sup>-3</sup>, and for optimal predator velocities,  $v_{max}$  (black line) and  $v_{min}$  (grey line) in the upper ( $z = 1$  m) (A) and (C) and lower of the surface mixed layer ( $z = 20$  m) (B) and (D). Temporal changes in prey concentration,  $Z_p$ , with varying wind for two different initial prey concentrations:  $10^5$  (E) and  $10^4$  m<sup>-3</sup> (F) at the upper ( $z = 1$  m) and lower of the surface mixed layer ( $z = 20$  m).

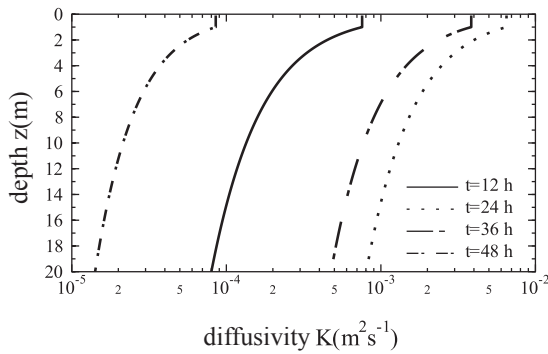


Fig. 9. Temporal changes in the vertical distributions of physical diffusivity,  $K$ .

of small body size  $d_o < 5.5$  mm and a high prey concentration  $Z_p > 10^7 \text{ m}^{-3}$ , the encounter velocity assumes low values (i.e.  $w < 0.01 \text{ m s}^{-1}$  for  $z = 1$  m) as in the case when  $l$  is defined as the Kolmogorov scale. In this situation, the choice of scale is not important for the encounter velocity obtained. Prey concentrations in the  $10^7 - 10^8 \text{ m}^{-3}$  range are reasonable densities for the prey of a 1-3 mm copepod (i.e. algae and protozoans). For large larval  $d_o > 10$  mm and prey concentrations lower than  $Z_p < 10^6 \text{ m}^{-3}$ , when  $l = f(Z_p)$  and  $l = f(d_o)$  the encounter velocity assumes high values in a like range (i.e.  $w > 0.015 \text{ m s}^{-1}$  for  $z = 1$  m); then the scale  $l$  can be defined as the average prey separation or as the predator's reactive distance. The larval lengths  $d_o > 10$  mm are mainly characteristic of the small sizes of freshwater species. However, for fish larvae in the 5-10 mm size range which feed on copepod nauplii in the  $10^4 - 10^5 \text{ m}^{-3}$  range, the encounter velocity assumes intermediate values i.e.  $0.01 < w < 0.015 \text{ m s}^{-1}$  when  $l = f(d_o)$ , which are higher than when  $l = f(\eta)$  and lower than when  $l = f(Z_p)$ . The results also demonstrate that the choice of scale significantly influences the encounter rate,  $E$ , through the turbulent encounter velocity,  $w$ . The calculations clearly indicate for which values of  $d_o$  and  $Z_p$  the encounter rate,  $E_{do}$  when  $l = f(d_o)$ , lies in the range  $E_\eta < E_{do} < E_{Zp}$ , i.e. between  $E_\eta$  when  $l = f(\eta)$  and  $E_{Zp}$  when  $l = f(Z_p)$ . For small larval sizes  $E_{do} \approx E_\eta$ ; however, for large ones  $E_{do} \approx E_{Zp}$ . In this paper, a normalized encounter rate, i.e. encounter rate,  $E$ , to behavioural encounter rate,  $E_B = E$  for  $U_{10} = 0$ , ratio, in the  $0 - 20 \text{ m s}^{-1}$  wind speed range was obtained for the analysis of the effect of turbulence on  $E$ . An increase in larval length as well as in prey density, when  $l = f(Z_p)$ , reduces the effect of turbulence on the encounter rate; however, when  $l = d$  and  $l = f(\eta)$ , the change in the prey concentration has no influence.

The intensity of this effect is to a high degree dependent on predator velocity,  $v$ . This intensity falls with rising predator velocity. The numerical investigations show that the choice of the length scale as well as the peculiarities of the individual investigated (i.e. a suitable definition of reaction distance and predator velocity) exert a great influence on the growth of predators through the encounter rate. The importance of the Kolmogorov scale,  $\eta$ , is greater in a laminar medium than in a turbulent medium.

In the quasi-laminar regime of water flow ( $l = 2\pi\eta$ ) and high prey concentration, the choice of correct scaling is not important. Predators of any body size forage in the same regime immovably (swimming velocity  $v \approx 0$ ).

In the second part of the paper, on the assumption that  $l = d$ , the effects of predator velocity and prey concentration on predator growth rate, when the predator is food limited, with a steady wind at various velocities were explored. Lastly, the time-dependent vertical distributions of predator growth rate, predator biomass and prey concentration with variable winds were examined (assuming an increase and then a decrease in wind speed during 2 days). The numerical studies were carried out on the basis of a one-dimensional prey-predator ecosystem model in which the dynamics of the horizontally quasi-homogeneous surface mixed layer were investigated. The calculations indicate that the predator growth rate de-

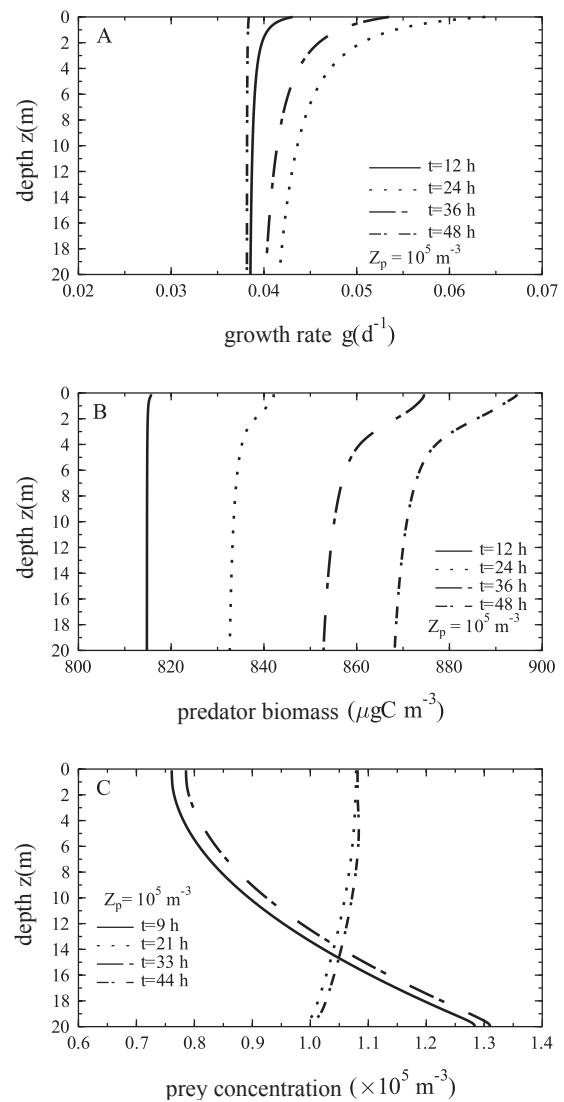


Fig. 10. Temporal changes in the vertical distributions of predator growth rate,  $g$ , (A), predator biomass,  $B$  (B) and prey concentration,  $Z_p$ , (C) during the period of numerical investigation (2 days), assuming the initial values of  $B = 800 \text{ } \mu\text{gC m}^{-3}$  and  $Z_p = 10^5 \text{ m}^{-3}$ .

depends to a significant degree on the prey concentration,  $Z_p$ , and predator velocity,  $v$ . Their increase in value causes a rise in predator biomass through an increase in its growth rate. However, the temporal increase in growth rate is considerable when winds are strong but falls with depth. For  $Z_p = 10^5 \text{ m}^{-3}$ , predator growth rate,  $g$ , depends on encounter rate ( $g_1 E$ ) and constant growth rate term ( $g_2$ ) and  $g_1 E \approx g_2$  when wind speed is low, but when one is high,  $g_1 E \gg g_2$  and  $g \rightarrow g_{\text{max}}$ . However, for  $Z_p = 10^4 \text{ m}^{-3}$ , the predominant influence of parameter  $g_2$  on growth rate is observed and then  $g \rightarrow g_2$ . In this paper, for instance, for the value of  $w = 0.005 \text{ ms}^{-1}$ , when  $U_{10} = 8 \text{ ms}^{-1}$ ,  $d_o = 7.5 \text{ mm}$  and  $l = d = f(d_o)$  and  $Z_p = 10^5 \text{ m}^{-3}$ , predator growth rate, when  $g_2 = 0.02 \text{ d}^{-1}$ , is ca.  $0.045 \text{ d}^{-1}$  and  $0.039 \text{ d}^{-1}$  for  $v_{\text{max}}$  and  $v_{\text{min}}$ , respectively. This means that the parameter  $g_2$  is about 35% for  $v_{\text{max}}$  and 41% for  $v_{\text{min}}$ , for *Mysis mixta* earlier stages (7.5 mm) feeding on copepods nauplii, assum-

ing that 80% of ingested food contributes to predator growth. The temporal changes in the vertical distributions of predator biomass reflect the growth rate, showing a strong turbulence-effect in the surface mixed layer, which increases with wind speed and decreases with depth. For a low prey density  $Z_o < Z_p < 10^4 \text{ m}^{-3}$  (where  $Z_o$  is prey threshold for predator growth) this effect disappears, and then the initial predator biomass and constant growth rate term have a decisive influence on prey concentration. However, the effect of turbulence on the characteristics investigated increases with increasing  $Z_p$ , and then the dominant factors controlling prey concentration are diurnal migration and predator growth rate in this case dependent mainly on encounter rate.

The 1D-model used in this paper consists of coupled, partial second-order differential diffusion-type equations for both predator and prey. Hence, this model was utilized in numerical investigations of the temporal changes in the vertical distributions of prey concentration and predator biomass. The temporal changes in the prey concentration,  $Z_p$ , are defined by turbulent diffusion, diurnal migration and predation. However, the temporal changes in the predator biomass are caused by turbulent diffusion and predator growth rate. The one-dimensional prey-predator ecosystem model presented here differs from the one given by (5). This is because

1. Davis' model [5], although also a 1D-model, determines the temporal changes in the horizontal distribution of predator biomass;
2. In this model, the diurnal migration of prey and predation were not considered, i.e. the effect of predator growth rate through predation on prey density was not studied; however, the swimming diffusivity for predator was considered;
3. Davis' model is based on a simplified version of the turbulent encounter rate equation given by [1];
4. Physical diffusivity and energy dissipation were defined by other equations. In this prey-predator model, the swimming diffusivity was not considered therefore the results of numerical simulations for predator biomass were different from those given by [5].

The results of the numerical investigations, achieved on the basis of the 1D-model presented in this paper, indicate that taking Eq. (4) into consideration for the encounter rate in Eq. (11), which describes the temporal variations in predator distribution, through the predator growth rate, is an important aspect of modeling the zooplankton concentration, for example, in the 1D upper layer model with a high-resolution zooplankton (herbivorous copepods) module [33, 44].

### Appendix 1

#### Parameters of the Eq. (9)

The temporal changes in mass (= weight) are caused by ingestion ING, zooplankton fecal pellets FEC and metabolism MET. The ingestion rate ING is defined as the rate of food in-

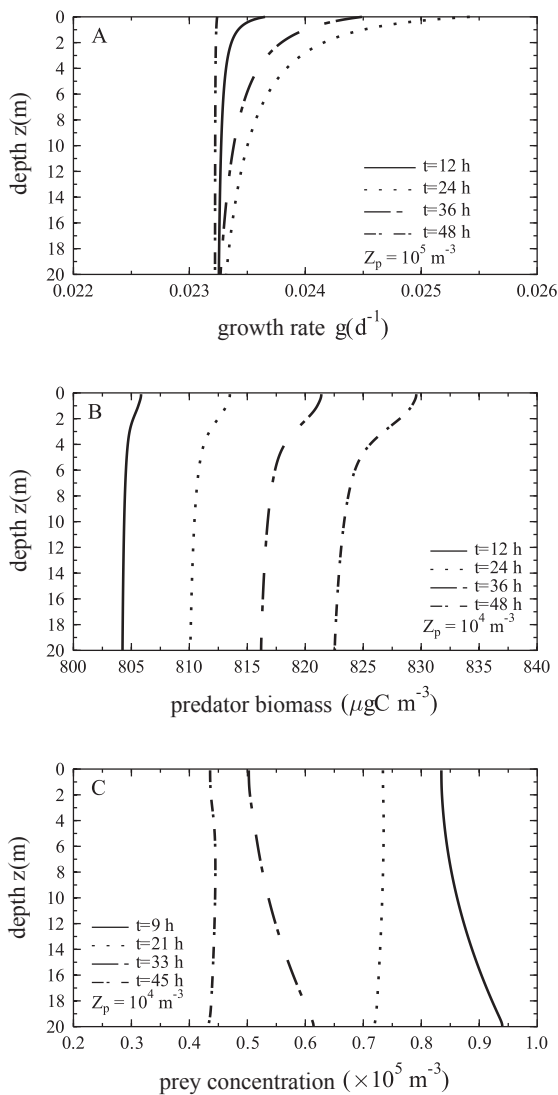


Fig. 11. Temporal changes in the vertical distributions of predator growth rate,  $g$ , (A), predator biomass,  $B$  (B) and prey concentration,  $Z_p$ , (C) during the period of numerical investigation (2 days), assuming the initial values of  $B = 800 \text{ µgC m}^{-3}$  and  $Z_p = 10^4 \text{ m}^{-3}$ .

take per unit time per animal, the coefficient of food selection being given by  $\tau$ . This function  $fil(\{Phyt\})$  with the maximal ingestion rate  $f_{\max}$  is a function of both the food concentration  $\{Phyt\}$  and the animal's weight  $W_p$ , and takes a value of  $\alpha$ , which is equal to 0.7 [45]. The allometric law ( $W_p^\alpha$ ) is determined experimentally by analyzing the total growth of the copepod. This signifies that the ingestion rate per unit weight decreases as weight increases [45]. This empirical relation is due to complex genetical and physiological phenomena occurring as the individual grows older, and is quite often used in models [44]. The total rate of metabolic loss MET can be split into three components with different relations to the food uptake rate ING.  $M_s$  is assumed to be the resultant or basic metabolism, independent of food supply. The respiratory costs of foraging for and capturing food  $M_R$  should fall as the food concentration and, correspondingly,  $f(\{Phyt\})$ , rises. Finally, there is the cost of assimilating and biochemically transforming the food (specific dynamic action,  $M_A$ ), proportional to  $A$  with a percentage of ingestion regenerated as soluble excretion zooplankton  $n_e$  [46]. The rate of assimilation  $A$  is computed as a constant fraction of the ingestion rate, e.g. [47], who used  $A = 0.7 \text{ ING}$ .

$$\text{ING} = \tau \text{fil}(\{Phyt\}) W_p^\alpha \quad (14)$$

$$\text{fil}(\{Phyt\}) = \text{fil}_{\max} (\{Phyt\} - \{Phyt_o\}) \setminus (\{Phyt\} - \{Phyt_o\} + k_{\text{phyt}}), \text{ for } \{Phyt\} > \{Phyt_o\} \quad (15)$$

$$\text{MET} = M_s + M_R + M_A = M_s + n_e A, A = n_a \text{ING} \quad (16)$$

$$\text{FEC} = n_j \text{ING} \quad (17)$$

## References

- ROTHSCHILD B.J., OSBORN T.R. Small-scale turbulence and plankton contact rates. *J. Plankton Res.* **10**, 465, **1988**.
- MACKENZIE B.R., MILLER T.J., CYR S., LEGGETT W.C. Evidence for a dome shaped relationship between turbulence and larval fish ingestion rates. *Limnol. Oceanogr.* **39**, 1790, **1994**.
- DOWER J., MILLER T.J., LEGGETT W.C. The role of microscale turbulence in the feeding ecology of larval fish. *Adv. Marine Biol.* **31**, 169, **1997**.
- SUNDBY S., FOSSUM P. Feeding conditions of Arcto-Norwegian cod larvae compared with the Rothschild-Osborn theory on small-scale turbulence and plankton contact rates. *J. Plankton Res.* **12**, 1153, **1990**.
- DAVIS C.S., FLIERL G.R., WIEBE P.H., FRANKS P.J.S. Micropatchiness, turbulence and recruitment in plankton. *J. Mar. Res.* **49**, 110, **1991**.
- MACKENZIE B.R., LEGGETT W.C. Quantifying the contribution of small-scale turbulence to the encounter rates between larval fish and their zooplankton prey: effects of wind and tide. *Mar. Ecol. Prog. Ser.* **73**, 149, **1991**.
- KIØRBOE T., SAIZE E. Planktivorous feeding in calm and turbulent environments with emphasis on copepods. *Mar. Ecol. Prog. Ser.* **122**, 135, **1995**.
- CAPARROY P., CARLOTTI F. A model for *Acartia tonsa*: effect of turbulence and consequences for the related physiological processes. *J. Plankton Res.* **18**, 2139, **1996**.
- BROWMAN H.I., SKIFTESVIK A.B. Effects of turbulence on the predation cycle of fish larvae: comments on some of the issues. *Mar. Ecol. Prog. Ser.* **139**, 309, **1996**.
- EVANS G.T. The encounter speed of moving predator and prey. *J. Plankton Res.* **11**, 415, **1989**.
- YAMAZAKI H., OSBORN T.R., SQUIRES K.D. Direct numerical simulation of planktonic contact in turbulent flow. *J. Plankton Res.* **13**, 629, **1991**.
- SEURONT L., SCHMITT F., LAGADEUC Y. Turbulence intermittency, small-scale phytoplankton patchiness and encounter rates in plankton: where do we go from here? *Deep Sea Res. I* **48**, 1199, **2001**.
- LOUGH R.G., MOUNTAIN D.G. Effect of small-scale turbulence on feeding rates of larval cod and haddock in stratified water on Georges Bank. *Deep-Sea Res. II* **43**, 1745, **1996**.
- GERRITSEN J., STRICKLER J.R. Encounter probabilities and community structure in zooplankton: a mathematical model. *J. Fish Res. Bd. Can.* **34**, 73, **1977**.
- MACKENZIE B.R., KIØRBOE T. Turbulence-enhanced prey encounter rates in larval fish: effects of spatial scale, larval behaviour and size. *J. Plankton Res.* **17**, 2319, **1995**.
- LAURENCE G.C. A report on the development of stochastic models of food limited growth and survival cod and haddock larvae. In: LAURENCE G.C., LOUGH R.G. (Eds.) Growth and survival of larval fish in relation to the trophodynamics of Georg Bank cod and haddock. NOAA Technical Memorandum NMFS F/NEC-36, Woods Hole, MA, pp. 83-150, **1985**.
- MILLER T.J., CROWDER L.B., RICE J.A., MARSHALL E.A. Larval size and recruitment mechanisms in fishes: toward a conceptual framework. *Can. J. Fish. Aquat. Sci.* **45**, 1657, **1988**.
- KIØRBOE T., VISSER A.W. Predator and prey perception in copepods due to hydromechanical signals. *Mar. Ecol. Prog. Ser.* **179**, 81, **1999**.
- JACKSON G.A., LOCHMANN S. Modelling coagulation of algae in marine ecosystems. In: BUFFLE J., VAN LEEUWEN H.P. (Eds.), Environmental Analytical and Physical Chemistry Series, 2, Environmental Particles. Lewis Publishers, Boca Raton, pp. 387-414, **1993**.
- DELICHATSIONS M.A., PROBSTEIN R.F. Coagulation in turbulent flow: theory and experiment. *J. Coll. Interf. Sci.* **51**, 394, **1975**.
- HILL P.S., NOWELL A.R.M., JUMARS P.A. Encounter rate by turbulent shear of particles similar in diameter to the Kolmogorov scale. *J. Mar. Res.* **50**, 643, **1992**.
- KIØRBOE T. Turbulence, phytoplankton cell size, and the structure of pelagic food webs. *Adv. Mar. Biol.* **29**, 1, **1993**.
- SUNDBY S., ELLERTSEN B., FOSSUM P. Encounter rates between first-feeding cod larvae and their prey during moderate to strong turbulence. *ICES Mar. Sci. Symp.* **198**, 393, **1994**.
- SUNDBY S. Wind climate and foraging of larval and juvenile Arcto-Norwegian cod (*Gadus morhua* L.). *Can. Spec. Publ. J. Aquat. Fish Sci.* **121**, 405, **1995**.

25. GALLAGHER B.R., BURDICK J.E. Mean separation distance of organisms in three dimensions. *Ecology* **51**, 538, **1970**.
26. MUELBERT J.H., LEWIS M.R., KELLEY D.E. The importance of small-scale turbulence in the feeding of herring larvae. *J. Plankton Res.* **16**, 927, **1994**.
27. DENMAN K.L., GARGETT A.E. Biological-physical interactions in the upper ocean: the role of vertical and small scale transport processes. *Annu. Rev. Fluid Mech.* **27**, 225, **1995**.
28. LEWIS D.M., PEDLEY T.J. Planktonic contact rates in homogeneous isotropic turbulence: theoretical predictions and kinematic simulations. *J. Theor. Biol.* **205**, 377, **2000**.
29. MANN J., OTT S., PÈCSELI H.L., TRULSEN J. Predator-prey encounters in turbulent waters. *Phys. Rev. E* **65**, 026304/1-4, **2002**.
30. YOUNG I.R., BANNER M.L. Modelling of finite depth wind wave dissipation, ONR Report, **2001**, WWW Page <http://www.onr.navy.mil/scitech/ocean/reports/dos/cd/01/cdyoun02.pdf>, **2001**
31. MASSEL S.R. Ocean surface waves: their physics and prediction. *Ad. Ser. Ocean Engineering*, **11**. World Scientific Publ. Singapore, **1996**.
32. DZIERZBICKA-GŁOWACKA L. Mathematical modelling of the biological processes in the upper layer of the sea. *Diss and monogr* **13**, Institute of Oceanology PAS, Sopot (in Polish), **2000**.
33. DZIERZBICKA-GŁOWACKA L. A numerical investigation of phytoplankton and *Pseudocalanus elongatus* dynamics in the spring bloom time in the Gdańsk Gulf. *J. Marine Sys.* **53**, 19, **2005**.
34. MACKENZIE B.R., KIRBOE T. Larval fish feeding and turbulence: A case for the downside. *Limnol. Oceanogr.* **45**, 1, **2000**.
35. OSBORN T.R. Estimates of the local rate of vertical diffusion from dissipation measurements. *J. Phys. Oceanogr.* **10**, 83, **1980**.
36. GREGG M.C. Scaling turbulent dissipation in the thermohaline. *J. Geophys. Res.* **94**, 9684, **1989**.
37. BURCHARD H. On the  $q^{21}$  equation by Mellor and Yamada [1982]. *J. Phys. Oceanogr.* **31**, 1377, **2001**.
38. JANKOWSKI A. Mathematical modeling of water circulation in the Baltic Sea. *Ossolineum, Polish Academy of Sciences*, pp. 1-275, **1988**.
39. SKIVESFIK A.B., HUSE I. Behaviour studies of cod larvae, *Gadus morhua* L. *Sarsia* **72**, 367, **1987**.
40. WITEK Z. Biological production and its utilization within a marine ecosystem in the western Gdańsk Basin. *Sea Fisheries Institute, Gdynia, Poland*, pp. 1-145, **1995**.
41. CISZEWSKI P., WITEK Z. Production of older stages of copepods *Acartia biflosa* Giesb. and *Pseudocalanus elongatus* Boeck in Gdansk Bay. *Pol. Arch. Hydrobiol.* **24** (4), 449, **1977**.
42. DZIERZBICKA-GŁOWACKA L. Growth and development of copepodite stages of *Pseudocalanus* spp. *J. Plankton Res.* **26**, 49, **2004a**.
43. DZIERZBICKA-GŁOWACKA L. The dependence of body weight in copepodite stages of *Pseudocalanus* spp. on variations of ambient temperature and food concentration. *Oceanologia* **46**, 45, **2004b**.
44. CARLOTTI F., RADACH G. Seasonal dynamics of phytoplankton and *Calanus finmarchicus* in the North Sea as revealed by a coupled one-dimensional model. *Limnol. Oceanogr.* **41**, 522, **1996**.
45. PAFFENHÖFER G.A. Grazing and ingestion rates of nauplii, copepodids and adults of the marine planktonic copepod *Calanus helgolandicus*. *Mar. Biol.* **11**, 286, **1971**.
46. STEELE J.H., MULLIN M.M. Zooplankton dynamics. In: GOLDBERG E.D., MCCAVE I.N., O'BRIEN J.J., STEELE J.H. (Eds.) *The sea*, **6**. Interscience Publ. New York, London, Sydney, Toronto, **1977**.
47. STEELE J.H. *The Structure of Marine Ecosystems*. Harvard University Press, Cambridge, **1974**.
48. DZIERZBICKA-GŁOWACKA L., ZIELIŃSKI A. Potential rate of reproduction for some geographically separate populations of *Pseudocalanus* spp. *Oceanologia* **46**, 65, **2004**.
49. RENK H., OCHOCKI S., PYTEL H. Short-term variations of primary production and chlorophyll in the Gdańsk Deep. *Pol. Ecol. Stud.* **9**, 341, **1983**.